Bulletin of the Disaster Prevention Research Institute, Vol. 15, Part 3, No. 103, March, 1966

Underwater Acoustic Telemetry for Oceanographical and Limnological Research (Part II)

By Seiichi KANARI

(Manuscript received January 13, 1966)

Abstract

The acoustic telemetry system described in this paper is designed for measuring depth, water temperature and turbidity in a reservoir. This instrument is self-contained and transmits a modulated super sonic F-M signal to a hydrophone near the shore or the surface of the reservoir. The transmitted signal is received and then demodulated to recover the original information for depth, water temperature and turbidity by a specially designed F-M receiver, and recorded on a D. C. recorder.

The system is completely acoustical and eliminates the need for electrical cables or other connecting devices. This can be also used for oceanographical observations in deep sea.

1. Introduction

The first model of the underwater acoustic telemetry system was constructed by the author in 1962 and tested in December, 1963. Though the device could not transmit an acoustic signal of more than 50 meter range because of the low power output, the vertical temperature distribution was telemetered and recorded with considerable accuracy.

In this paper, an improved model is described, which has five channels ; depth, water temperature, turbidity and two references. The underwater transmitter contains five subcarrier oscillators as shown in figure 1. Three of them generate sine wave signals and their frequencies vary from 240 to 420 cps according to each piece of information of water temperature, depth and turbidity respectively within the following ranges : water temperature ; 10~30°C, depth (in hydrostatic pressure) ; 0~50 kg/cm^2, turbidity (in silt concentration) ; 0.1~3.0 g/l. The other two generate the reference signals with constant frequency of 241 cps and 420 cps respectively. These signals are selected successively by a mechanical commutator, and they modulate the frequency of 40 kc maincarrier, which is emitted through a sound signal projector as a super sonic wave after amplification of electrical power. The model contains an additional remote control switching system which extends the battery life considerably. When a sound pulse train of 71 kc is emitted at the receiving station and transmitted to the underwater transmitter, the sound pulse train is converted into an electric pulse train through the receiving transducer mounted on the underwater transmitter, and the pulse train is amplified and then it triggers the flip-flop circuit and switches the self-contained power source on. This state is retained until the next pulse train again triggers the flip-flop circuit, and by this second pulse train, the flip-flop

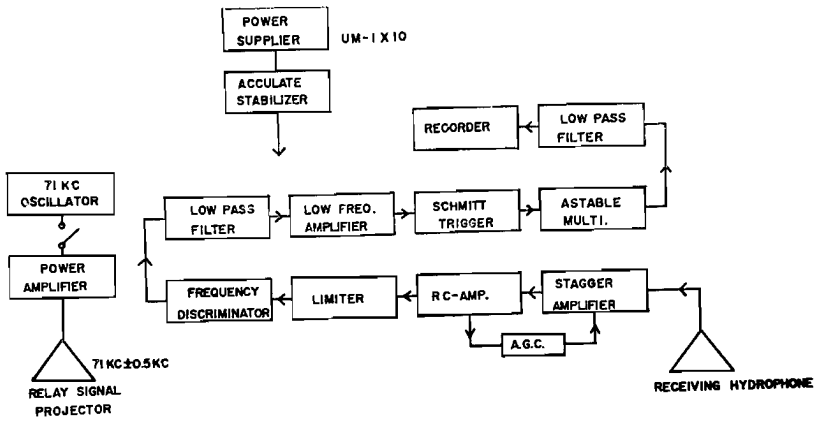

Fig. 1 (a). The block diagram of the deck unit of the underwater acoustic telemetry system.

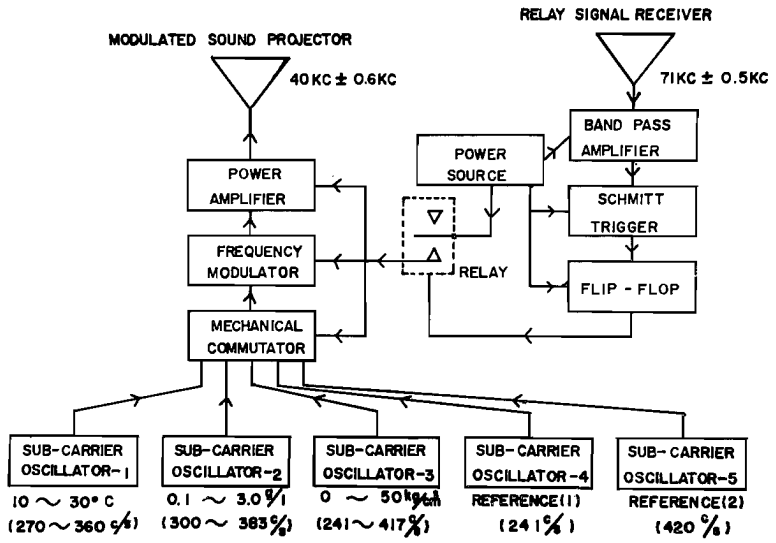

Fig. 1 (b). Block diagram of the underwater transmitter.

circuit returns to its initial state and the circuit of power supplier is open.

The electrical design and construction of the improved model are described in the following chapters in detail and some results of a test, carried out in Amagase reservoir in December, 1965, are also shown in the last chapter.

2. Underwater transmitter

a) Subcarrier oscillator for temperature measurement

Water temperature is measured by means of a thermister bridge as shown in figure 2. Output voltage of this bridge varies linearly from −100 to +200 mv in accordance with temperature change between 10 and 30°C, and is applied to the input terminals 1 and 2 of the oscillator of voltage control type whose

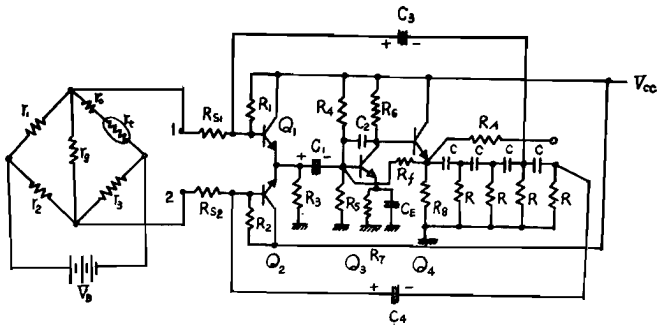

$R_{S_1} = R_{S_2} = 50K$
$R_1 = R_2 = 200K$
$R_3 = 10K$
$R_4 = 100K$
$R_5 = 1CK$
$R_6 = 5K$
$R_7 = 2K$
$R_f = 100K$
$R_8 = 2K$

$C_1 = 3\mu F$
$C_2 = 0.002\mu F$
$C_3 = C_4 = 3\mu F$
$C_E = 20\mu F$
$C = 0.05\mu F$
$R = 5K$
$R_A = 8K$

$Q_1 = Q_2 = \mu pA\text{-}15$
$Q_3 = Q_4 = 2SC\text{-}284J.$
$r_0 = 7K$
$r_1 = 27K$
$r_2 = 8.2K$
$r_3 = 5K$
$r_g = 6.2K$
$V_B = 9.2V$
$V_{cc} = 10V$
r_t = thermister

Fig. 2. Schematic circuit diagram of the subcarrier oscillator for temperature measurement.

frequency varies from 270 to 360 cps according to the bridge output between −100 and +200 mv. The overall characteristics of the temperature sensitive subcarrier oscillator is shown in figure 4 (a). Over a temperature range from 10 to 30°C, a frequency fluctuation of 1 cps was observed in laboratory test and this tells that the accuracy of temperature determination is about one per cent.

b) Subcarrier oscillator for pressure measurement

The subcarrier oscillator is shown in figure 3. The bridge contained in the oscillator is in resistive balance in the atmosphere, and when water pressure

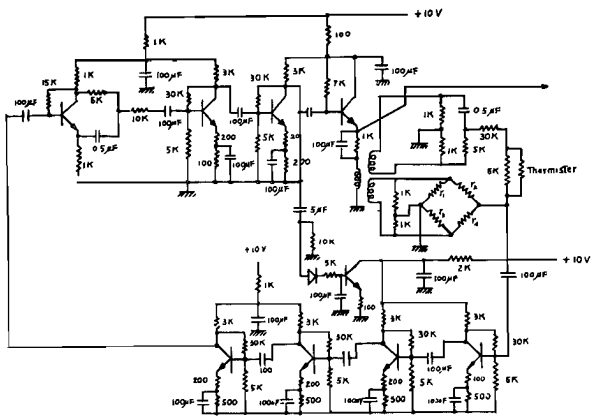

Fig. 3. Schematic circuit diagram of the sobcarrier oscillator for pressure measurement.

is applied to the pressure transducer, the pressure sensitive diaphragm is distorted and it results in an unbalance in the bridge circuit which consits of three constant resistances r_1, r_2, r_3 and one strain gauge r_4 whose resistance varies with the distortion of diaphragm. The resultant unbalance in the bridge circuit produces a phase shift to the positive feed-back current in the oscillator circuit, and it controls the output frequency from 210 to 400 cps in accordance with the pressure change from 0 to 50 kg/cm^2. A calibration curve of pressure vs output frequency of the subcarrier oscillator in laboratory test is shown in figure 4 (b). The output frequency is thus a linear function of the pressure, applied to the diaphragm, and overall accuracy was estimated at about 1.5 per cent.

c) Subcarrier oscillator for turbidity measurement

Turbidity is measured as the relative absorption of light which is transmitted horizontally through the water from a light source with constant strength. The transmission range of the ray is about 10 cm and the output current of the photo-electric transducer, which consists of a P-N junction Silicon Photo Cell, is 2.5 milliamperes in clear water (distilled water) and it decreases as the suspended silt concentrations increase. The output current is applied to the same oscillator as the subcarrier oscillator for temperature measurement, whose frequency varies from 300 to 370 cps in accordance with turbidity (suspended silt concentration). Figures 4 (c) and 5 show the characteristics

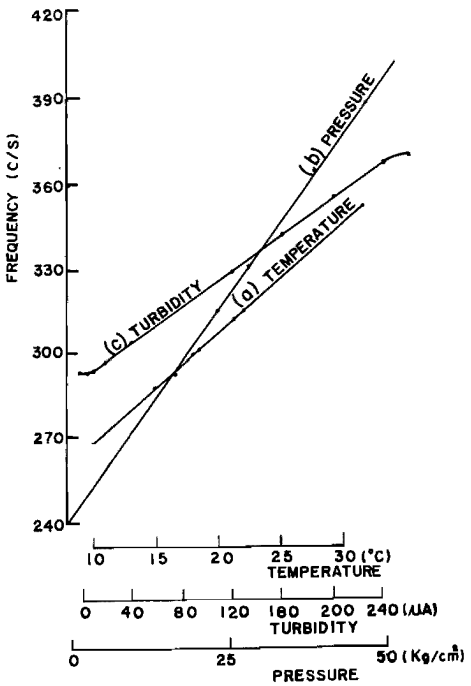

Fig. 4. Calibration curves of the measured quantities vs. output frequencies each subcarrier oscillator.

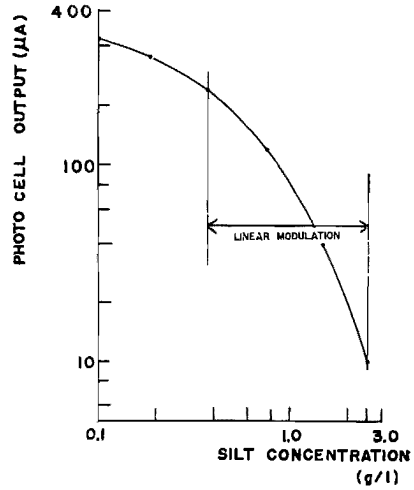

Fig. 5. Calibration curve of silt concentration vs. output current of the photo-electric cell.

of the subcarrier oscillator measured in laboratory by using the silt picked up at Amegase reservoir.

d) Oscillators of reference signals

The subcarrier oscillator of reference signals are the same type as those for temperature measurement and they generate two constant frequencies of 241 cps and 420 cps respectively.

e) Commutator

The commutator in the underwater transmitter is stepping relay which is arranged to operate every 4.7 seconds at five position and select the output signals of five subcarrier oscillators in the following order :
The stepping relay is driven by micro-motor which consumes power of about 0.5 watts.

switch position	duration time	selected signal
1	4.7 sec	reference-2
2	4.7 〃	turbidity
3	4.7 〃	depth
4	4.7 〃	reference-1
5	4.7 〃	turbidity
6	9.4 〃	temperature

f) Maincarrier modulator

The output signal of subcarrier oscillators modulates the 40 kc maincarrier generated by the same oscillator of voltage control type as the subcarrier oscillator for temperature measurement, and the resultant output frequency varies from 39.55 to 40.75 kc in accordance with the amplitude of the subcarrie signals between +0.5 and −0.5 v. The maximum frequency deviation is about 1.56 % for the input voltage of 0.5 v and its modulation index m_f for each subcarrier signal are shown in Table 1.

TABLE 1.

channel	subcarrier	frequency	modulation index m_f	required max. spectrum band width (B_{max})
1	temp.	270 to 360 cps	1.66 to 2.22	10×420 cps= 4.2kc (±2.1 kc)
2	press.	240 to 420 cps	1.43 to 2.50	
3	turb.	300 to 380 cps	1.58 to 2.00	
4	refer.-1	241 cps	2.49	
5	refer.-2	420 cps	1.43	

The modulated main carrier signal is amplified through the driver stage and class B push-pull power amplifier to the power level of 4 watts, and then applied to the sound signal projector which converts the modulated electric power to the acoustic power and radiates the sound signals with the directivity as described in the next chapter.

3. Acoustic transducer

The acoustic transducer of the transmitter plays the important role of converting the electrical signal to an acoustic signal, because the modulated electric signal has a frequency spectrum between 38.5 and 41.5 kc approximately, and in order to transmit the accurate information, electric signal must be transduced to a sound signal through the acoustic transducer without any distortion. Consequently, it is desired that the acoustic transducer has a flat characteristics in regard to the frequency over the spectrum band width of ±2.1 kc. However, the cylindrical barium-titanate transducer (30 mm height, 38 mm dia. and 3 mm thick), used in the present model, also has a resonant frequency at about 40 kc and its Q-value is about 100 in air and 50 in water. In order to satisfy the requirement described above, the Q-value should be less than 19.3 (the center of main carrier frequency F_0 is 40.5 kc, and the side-band width of spectrum ΔF is 2.1 kc, therefore, $Q=\frac{F_0}{\Delta F}=19.3$). This requirement is satisfied by the sticking the inner face of the cylindrical transducer with foam rubber as shown in figure 6. By this method the Q-value of the transducer could be lowered to about 7, and the efficiency of the transducer is 20 per cent in the required frequency range, which was estimated by measuring the phase difference between the electric current and the voltage at the input terminals of the transducer immersed in the water. The vibration mode of this transducer is a radial-spreading vibration, consequently it shows a two-dimensional non-directivity pattern in the plane perpendicular to the axis of the cylinder. Such a directivity pattern is not economical for this model, because the receiving point is only one in the acoustic field ; it is favorable that the acoustic sound, emitted from the transducer, has a unidirectional pattern so that most of the sound energy might be received by a

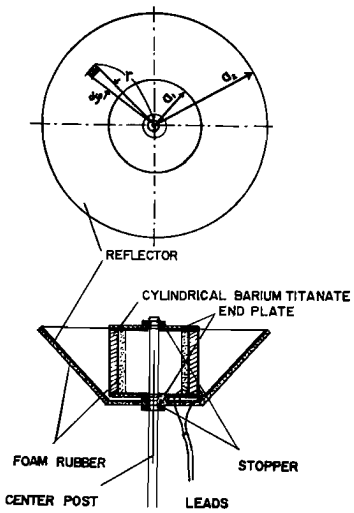

Fig. 6. Schematic diagram of the modulated sound projector.

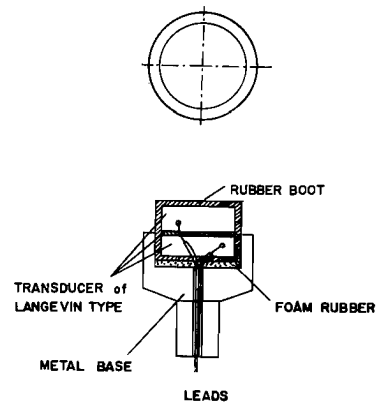

Fig. 7. Schematic diagram of the electro-acoustic transducer of Langevin type, used for the relay signal projector and the relay signal receiver.

hydrophone at the receiving station. For this purpose, the reflector is installed on the transducer as shown in figure 6. The directivity function R_1 is given by the following integral

$$R_1=\frac{1}{\pi(a_2^2-a_1^2)}\int_{a_1}^{a_2} r dr \int_0^{2\pi} e^{jK_1 r\cos\varphi\sin\theta} d\varphi \tag{1}$$

where, φ is the angle between the cylinder axis and the line passing through the center of cylinder and the observing point, and K_1 is a wave number of sound. The notations on a_1, a_2, r and θ are shown in figure 6.

Evaluating this integral, we obtain the following formula

$$R_1=\frac{2[\lambda_2 J_1(\lambda_2)-\lambda_1 J_1(\lambda_1)]}{\lambda_2^2-\lambda_1^2} \tag{2}$$

where, $\lambda_1=K_1 a_1\sin\theta$, $\lambda_2=K_1 a_2\sin\theta$ and $J_1(\lambda)$ is the first order Bessel function.

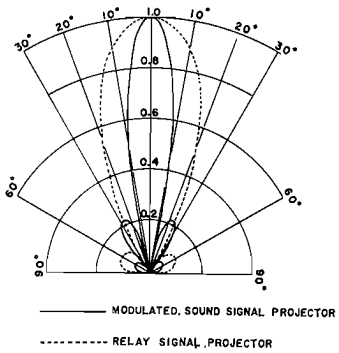

Fig. 8. Directivity patterns of the modulated sound projector and of the relay signal projector.

The electro acoustic transducer of Langevin type as shown in figure 7, were used for the relay signal projetor and for the relay signal receiver, with the resonant frequency of 71 kc. The directivity function R_2 of this transducer is given by the formula

$$R_2=\frac{2J_1(K_2 a\sin\theta)}{K_2 a\sin\theta} \tag{3}$$

where, a is the radius of this transducer, K_2 is a wave number of sound, θ and $J_1(\lambda)$ are the same notation as in eq. (1).

The directivity pattern of these sound projectors, computed from the values of $a_1=2.5$ cm, $a_2=7.5$cm, $K_1=1.675$, $a=4.0$ cm, and $K_2=3.14$, are shown in figure 8.

4. General description of deck unit

The deck unit consits of an F-M receiver and pulse generator for relay control. Figure 9 shows the circuit diagram of the F-M receiver in the deck unit. The 40 kc F-M signal which was picked up by a receiving hydrophone, is applied to a band pass amplifier $T_1\sim T_7$ and then after passing through the limiter $T_8\sim T_9$, the subcarrier signal is separated from the main carrier signal by the main carrier discriminator $T_{10}\sim T_{11}$. The resultant subcarrier signal is further amplified through $T_{12}\sim T_{16}$ and is applied to the monostable-multivibrator which generates the rectangular wave with the same frequency as that of the input subcarrier signal. Finally, the generated rectangular wave is rectified and converted to D. C. voltage which has a linear relation with the frequency of the input subcarrier signal ; the output D. C. voltage varies from 0.175 to 0.915 v in accordance with the frequency change of the subcarrier signal between 240 and 420 cps.

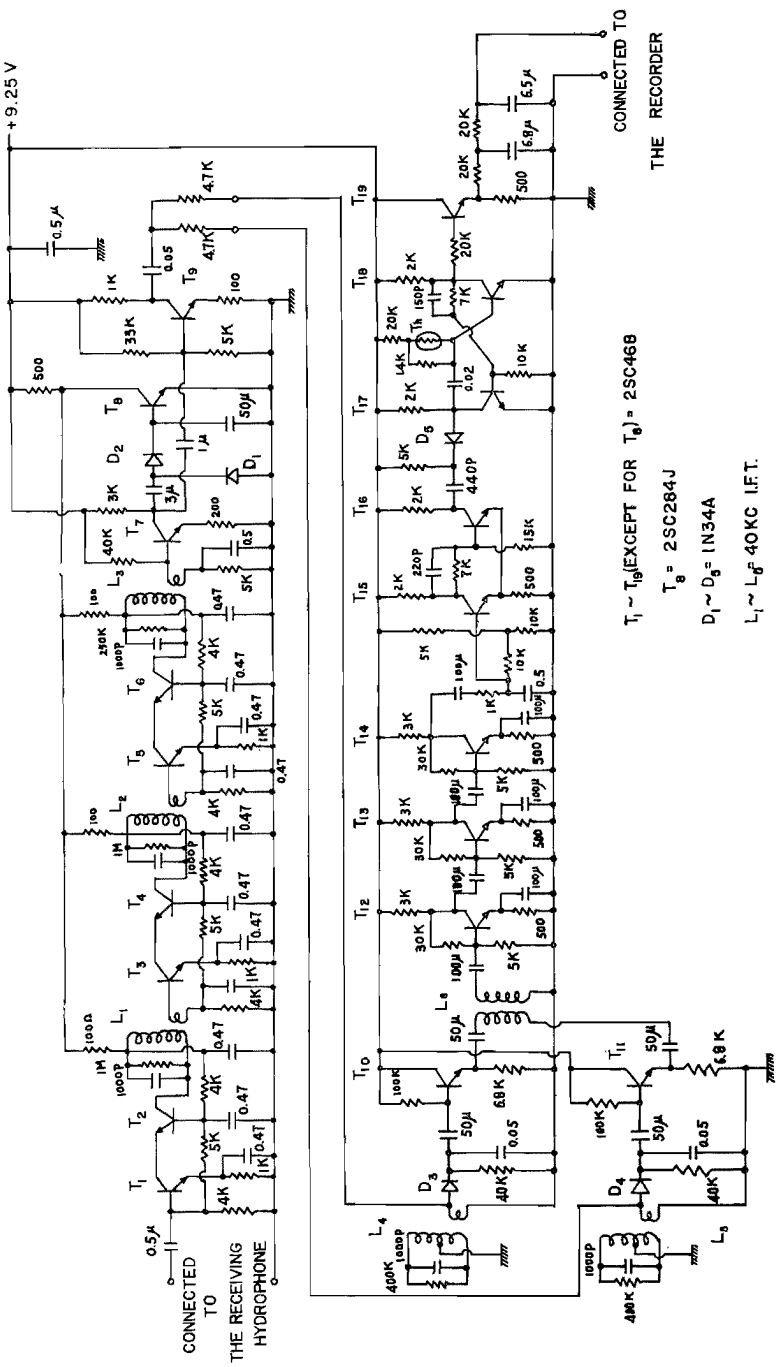

Fig. 9 S. chematic circuit daigram of the deck unit, excluding the relay control pulse generator.

5. Relay control circuit

An electric power of 12 watts is consumed in the transmitter and is supplied by eight series connected UM-1 dry batteries in three pararell connection, which have a life of 2.5 hours in the case of continuous operation. The flip-flop relay circuit, shown in the diagram of figure 1, is triggered by 71 kc sound pulse which is emitted from the remote control pulse generator consists of a Hartley type oscillator and a power amplifier. The output frequency of the oscillator is 71 kc and the output power of the power amplifier is about 4 watts, and acoustic total power is about 2.3 watts. The pulse emission is made by connecting the circuit between the oscillator and the power amplifier by means of a push-button switch. At any time the relay control system in the underwater transmitter is ready for responding to the control pulse emitted from the deck unit, and in this state the control circuit consumes the electric power of 0.96 watts.

As pointed out in the introduction of this paper, the remote control system permits the transmitter to be switched on and off in the ships or at the shore, and its function is primarily to save the consumption of battery power when the data recording is stopped.

6. Structural design

Photo. 1 shows a general view of the underwater transmitter. The electronic components assembly (photo. 2) is contained in the Alminium tube with 60 mm dia, 5.0 mm thick and 1.1 m long, and batteries are contained in the four slender tubes with 40 mm dia, 3.0 mm thick and 0.77 m long, arranged around the main tube, and they are fixed each other through the two circular plates. The sensers of temperature, pressure and turbidity are mounted on the lower end of the main tube, and the temperature senser in which the thermister is enclosed, is thermaly insulated from the main tube in order to minimize the thermal capacity of the senser. The structure of these sensers are shown in figures 10 and 11.

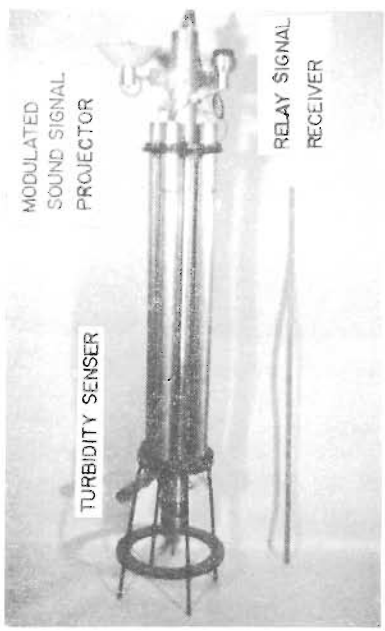

Photo. 1. General view of the underwater transmitter.

The sound projector of F-M signal and the receiver of relay control pulse are mounted on the upper side of the main tube.

Photo. 3 shows the deck unit assembly. The receiving hydrophone, the type of TAU-1 has the sensitivity of -108 *db* (0 *db*=1v/μ bar) at 40 kc, and was originally omnidirectional. As it is desirable that the receiving hydrophone has a directivity to some extent, a corn-shaped reflector similar to that of the modulated sound projector, was installed to the original hydrophone. The acoustic pro-

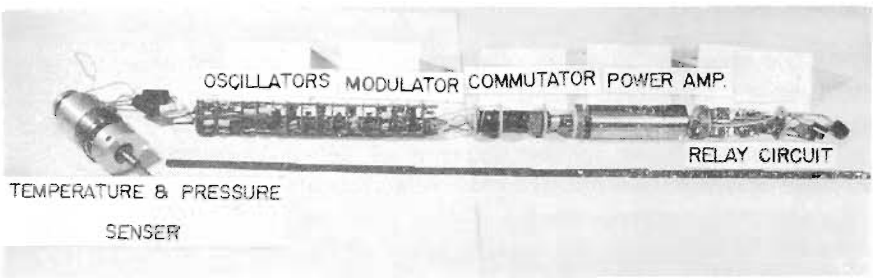

Photo. 2. Electronic component assembly of the underwater transmitter.

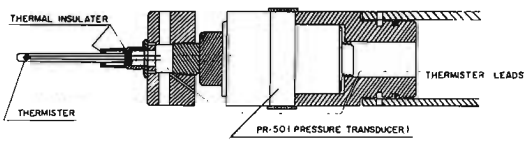

Fig. 10. The installation of thermister and pressure transducer.

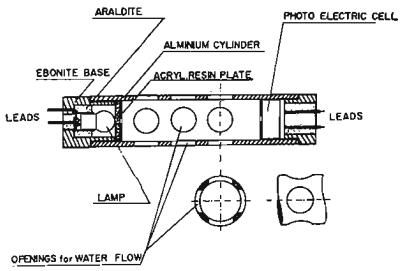

Fig. 11. Schematic diagram of the turbidity senser.

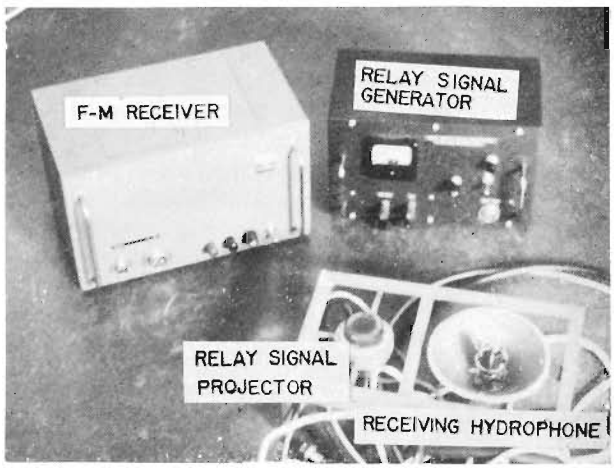

Photo. 3. General view of the deck unit assembly.

jector for relay control pulse emission is the same type as the relay control pulse receiver. The receiving hydrophone and the relay control pulse projector are installed on the frame whose angle of depression is variable between 0 and 90 degrees, consquently, we can set main axis of directivity of these transducers so as to receive the best signals.

7. Some results of tests

Figure 12 shows the record of the transmitted signals when temporary heat-

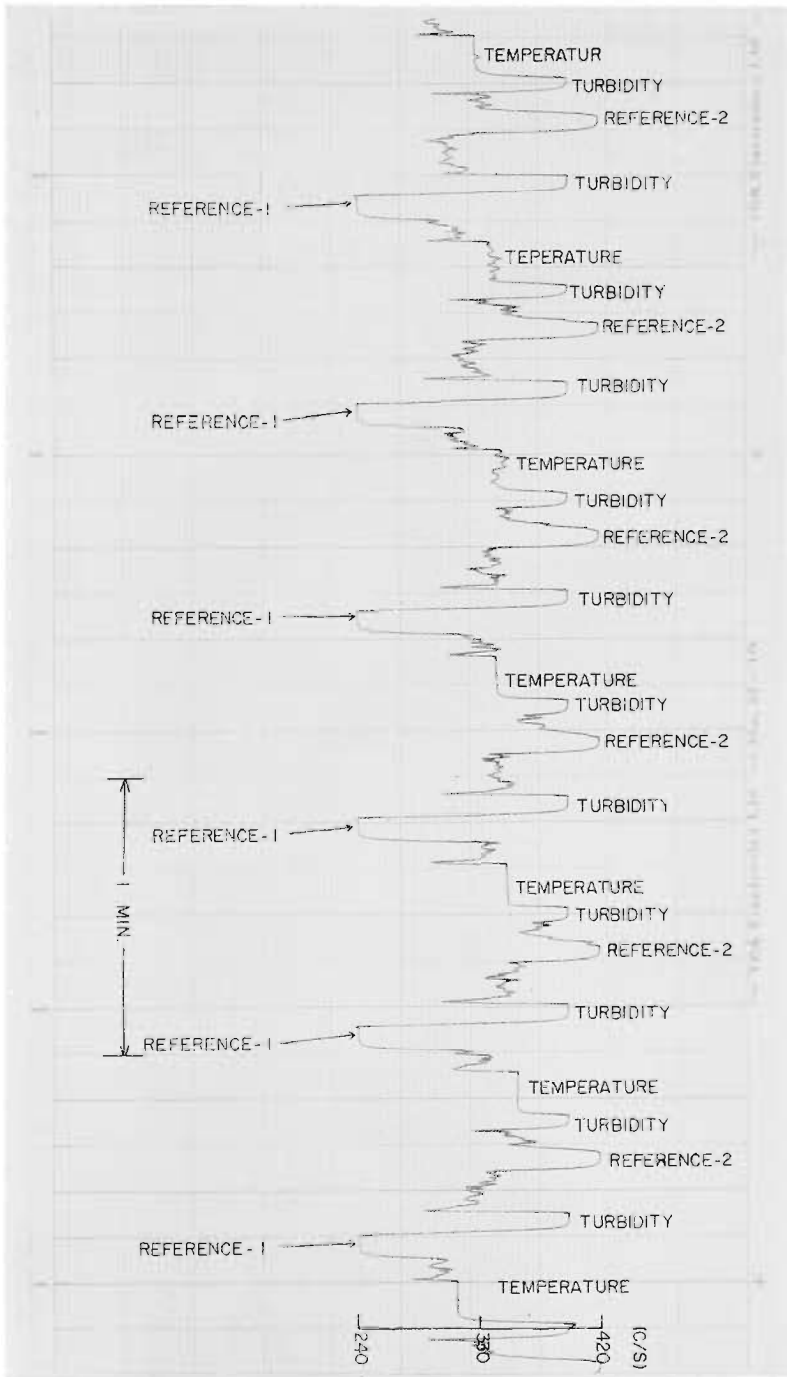

Fig. 12. A telemetered record when an artificial temperature change was given to the temperature senser in the atmosphere.

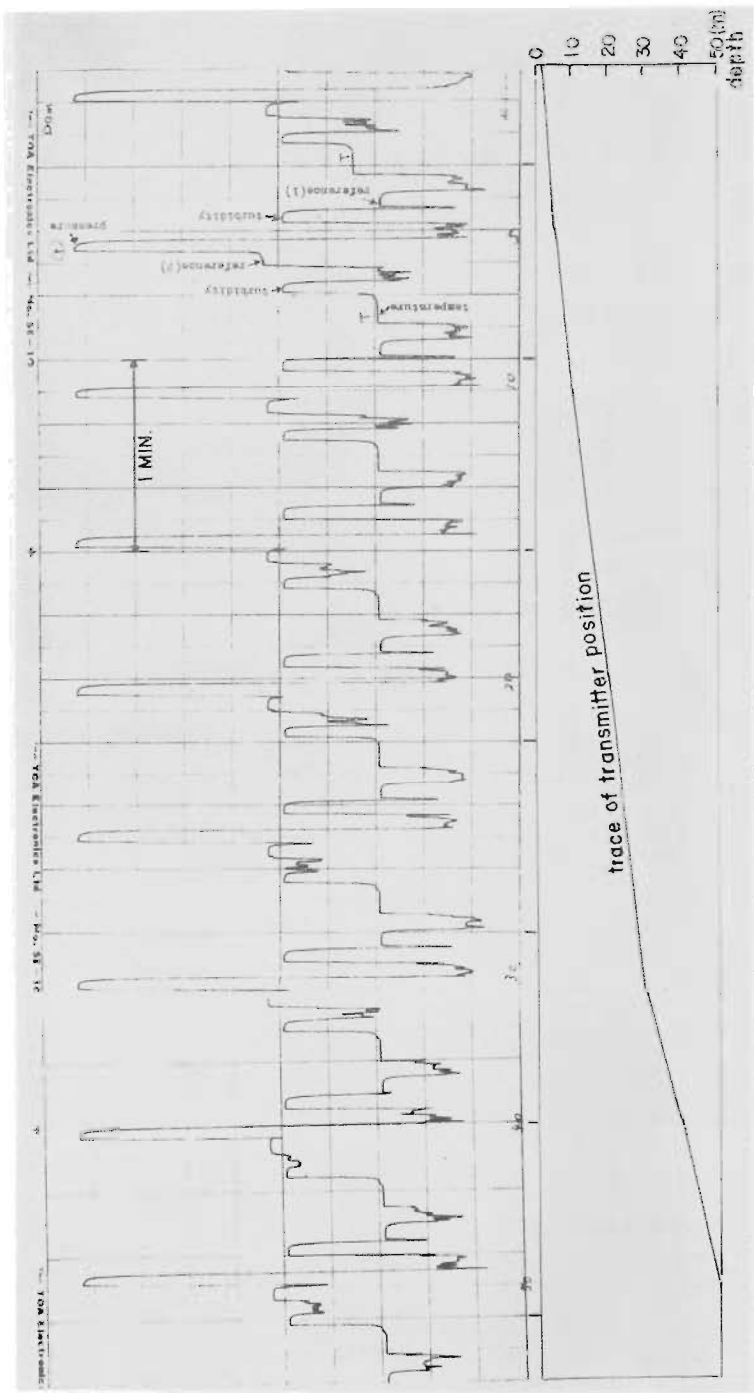

Fig. 13. An example of telemetered record when the transmitter was lowered slowly to the bottom layer of the reservoir.

ing and natural cooling were given to the temperature senser in the atmosphere. In the stage of natural cooling, some unstable temperature record appeared, which was due to a miss contact in the commutator relay, and except for this point, temperature change has been recorded fairly well. In this test, the pressure oscillator was excluded, therefore the position of the pressure signal is replaced by noise.

Field tests on the vertical and the horizontal transmission were carried out in Amagase reservoir in November, 1965. Figure 13 a typical example of record on the vertical transmission when the transmitter was lowered slowly to the bottom layer of the reservoir. Signals are recorded in the following order ; (1) reference-1, (2) turbidity, (3) depth, (4) reference-(2), (5) turbidity and (6) temperature. In this record, the pressure (depth) signal does not follow the transmitter displacement and shows a high frequency oscillation which is due to an abnormal high frequency oscillation of the subcarrier oscillator. Under normal conditions of the subcarrier oscillator, the pressure record must follow the pressure change in the range between two reference levels as

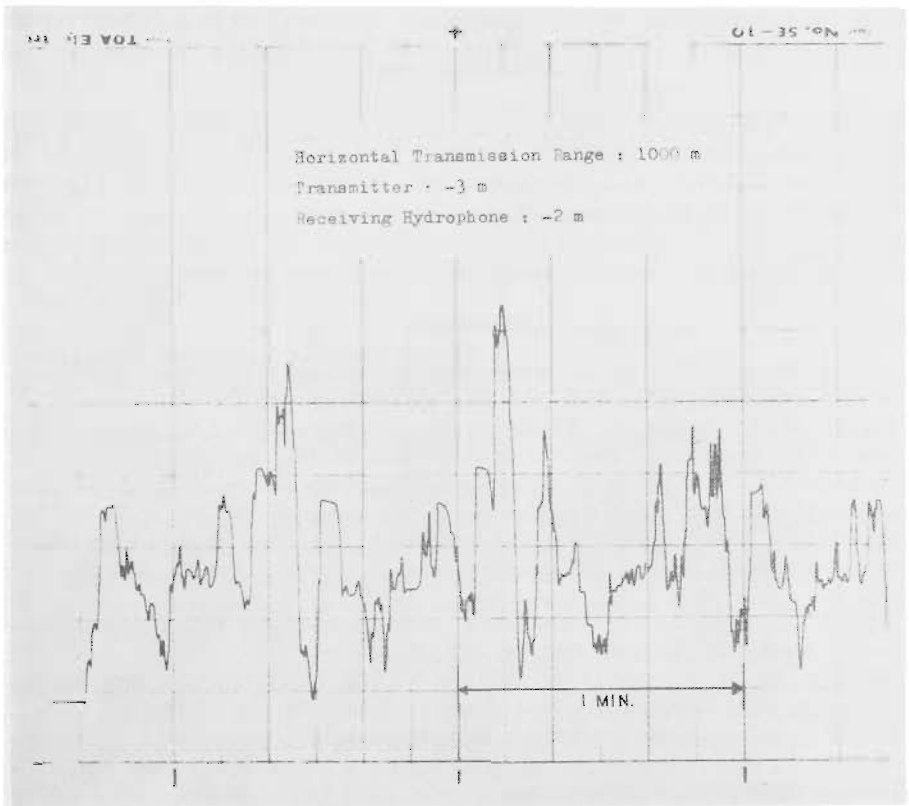

Fig. 14. A record obtained from the horizontal transmission test of 100 m range, conducted along the longitudinal way of the reservoir, setting the transmitter and the receiving hydrophone at the depths of 3 meters and 2 meters respectively below the water surface.

the transmitter is descending in the water. The depth of the descending transmitter was measured by the length of a suspended rope and is shown in the bottom of this figure.

The temperature record shows that the temperature gradient in the upper layer is about 2°C/m, and in the layer below 7 m it shows a very small gradient with 0.005°C/m. Turbidity record does not show any remarkable distribution during this test.

A horizontal transmission test was made along the longitudinal way of this reservoir, setting the transmitter and the receiving hydrophone at the depths of 3 meters and 2 meters below the water surface respectively, and keeping them at intervals of about 1000 meters. As shown in figure 14 the record of transmitted signal is very unstable because of the multi-path interferences from the bottom and the surface of the water. Though this instablity may vanish with increasing the depth of the transmitter or hydrophone, the multi-path interference restricts the use of this instrument within a narrow limit so far as horizontal transmission is concerned.

The author has scheduled to perform further experiments of this system for the deep sea observations, and the results will be described in a future report.

Acknowledgements

The author is greatly indebted to Dr. Setsuo Okuda and several members of the staff at the Disaster Prevention Research Institute of Kyoto University for their valuable criticism and encouragement throughout this study. He also extends his gratitude to all who took part in this study, and particularly to Mr. K. Ōhashi and Mr. S. Mihara of Hayakawa Electric Co. for their kind help in the construction of the electronic components of this equipment.

References

1) Beakley, W. R. : The design of thermistor thermometers with linear calibration, Journal of Scientific Instruments, Vol. 28, June, 1951, pp. 176–179.
2) Tucker, M. J., Bowers, R., Pierce, F. E., and Barrow, B. J. : An acoustically telemetering depth gauge, Deep-Sea Research, Vol. 10, 1963, pp. 471–478.
3) Paramonov, A. N. : The use of the the principles of discrete counting for the transmission of data from deep-sea measurements, Okeanologiya, Vol. No. 4, pp. 710–716.
4) Heindsmann, T. E., Smith, R. H., and Arneson, A. C. : Effect of Rain upon Underwater noise levels, Journal of Acoustic Society of America, Vol. 27, 1955 PP. 378–379.
5) Willard, D. : A telemetering hydrophone, Contribution of the Woods Hols Oceanographic Institution, No. 1130, 1960, pp. 142–147.
6) Officer, C. B. : Introduction to the theory of SOUND TRANSMISSION with application to the ocean, McGraw Hill Book Company, INC., 1958, pp. 146–184.
7) Albers, V. M. : Underwater acoustics, Prenum press, New York, 1961.
8) Stephens, F. H. Jr. : Underwater telemeter for trawl fishing, Electronics, March 27, 1959, pp. 66–68.
9) Campbell, D. E., Cyr, R. J., Crosier, C. : Underwater telemetry for oceanographic research, Electronics, January 12, 1962, pp. 53–55.